We have engineered transgenic mouse lines carrying the HCV genome where by introducing the genes from the cDNA of the HCV genome of genotype 1b (Moriya et al. 1997, 1998). Established are four different kinds of transgenic mouse lines, which carry the core gene, envelope genes, the entire nonstructural (NS) genes, and NS5A gene, respectively, under the same transcriptional regulatory element. Among these mouse lines, only the transgenic mice carrying the core gene developed HCC in two independent lineages (Moriya et al. 1998). The envelope gene transgenic mice do not develop HCC, despite high expression levels of both E1 and E2 proteins (Koike et al. 1995, 1997), and the transgenic mice carrying the entire NS genes or NS5A gene have developed no HCC.

The core gene transgenic mice, early in life, develop hepatic steatosis, which is one of the histologic characteristics of chronic hepatitis C, along with lymphoid follicle formation and bile duct damages. Thus, the core gene transgenic mouse model well reproduces the feature of chronic hepatitis C. Of note, any pictures of significant inflammation are not observed in the liver of this animal model. Late in life, these transgenic mice develop HCC. Notably, the development of steatosis and HCC has been reproduced by other HCV transgenic mouse lines, which harbor the entire HCV genome or structural genes including the core gene (Lerat et al. 2002; Machida et al. 2006; Naas et al. 2005). These outcomes indicate that the core protein *per se* of HCV has an oncogenic potential when expressed in vivo.

5 HCV Augments Oxidative Stress Production and Modulates Intracellular Signaling

There is a notable feature in the localization of the core protein in hepatocytes; while the core protein predominantly exists in the cytoplasm associated with lipid droplets, it is also present in the mitochondria and nuclei (Moriya et al. 1998). On the basis of this finding, the pathways related to these two organelles, the mitochondria and nuclei, were thoroughly investigated.

One effect of the core protein is an increased production of oxidative stress in the liver. We would like to draw particular attention to the fact that the production of oxidative stress is increased in the core gene transgenic mouse model in the absence of inflammation in the liver. The overproduction of oxidative stress results in the generation of deletions in the mitochondrial and nuclear DNA, an indicator of genetic damage (Moriya et al. 2001a).

Augmentation of oxidative stress is implicated in the pathogenesis of liver disease in HCV infection as shown by a number of clinical and basic studies (Farinati et al. 1995). Reactive oxygen species (ROS) are endogenous oxygen-containing molecules formed as normal products during aerobic metabolism. ROS can induce genetic mutations as well as chromosomal alterations and thus contribute to cancer development in multistep carcinogenesis (Fujita et al. 2008; Kato et al. 2001). Oxidative stress has been shown to be more augmented in hepatitis C

than in other types of hepatitis such as hepatitis B (Farinati et al. 1995). Thus, a major role in the pathogenesis of HCV-associated liver disease has been attributed to oxidative stress augmentation, but little has been known about the mechanism of increased oxidative stress in HCV infection. Hence, it is an important issue to understand the mechanism of oxidative stress augmentation, both on generation and scavenging of ROS, which may allow us to develop new tools of therapies for chronic hepatitis C.

Other pathways in hepatocarcinogenesis would be the alteration of the expression of cellular genes and modulation of intracellular signaling pathways. For example, tumor necrosis factor (TNF)-α and interleukin-1β have been found transcriptionally activated (Tsutsumi et al. 2002). The mitogen-activated protein kinase (MAPK) cascade is also activated in the liver of the core gene transgenic mouse model. The MAPK pathway, which consists of three routes, c-Jun N-terminal kinase (JNK), p38, and extracellular signal-regulated kinase (ERK), is involved in numerous cellular events including cell proliferation. In the liver of the core gene transgenic mouse model prior to HCC development, only the JNK route is activated. In the downstream of the JNK activation, transcription factor–activating protein (AP)-1 activation is markedly enhanced (Tsutsumi et al. 2002, 2003). At far downstream, the levels of cyclin D1 and cyclin-dependent kinase (CDK) 4 are increased. Thus, the HCV core protein modulates the intracellular signaling pathways and gives advantage for cell proliferation to hepatocytes. In addition, HCV core protein suppresses the expression of suppressor of cytokine signaling (SOCS)-1, a negative regulator of cytokine signaling pathway, which may work as a tumor suppressor gene (Miyoshi et al. 2005).

Such an effect of the core protein on the MAPK pathway, combined with that on oxidative stress, may explain the extremely high incidence of HCC development in chronic hepatitis C (Fig. 2).

6 Mitochondria as Origin of ROS Production in HCV Infection

What is the origin for the increase in oxidative stress in the liver of hepatitis C patients? The core protein is mostly localized to the endoplasmic reticulum (ER), but it is also localized to the mitochondria in cultured cells and transgenic mice (Moriya et al. 1998; Suzuki et al. 2005). In addition, the double structure of mitochondrial membranes is disrupted in hepatocytes of core gene transgenic mice. Evidence suggests that the core protein modulates some mitochondrial functions, including fatty acid β-oxidation, the impairment of which may induce lipid abnormalities and hepatic steatosis. In addition, the mitochondrion is an important source of ROS. In livers of transgenic mice harboring the core gene, increased ROS production has been observed (Moriya et al. 2001a). A recent study found, by the proteomic profiling of biopsy specimens, that impairment in key mitochondrial processes, including fatty acid oxidation and oxidative

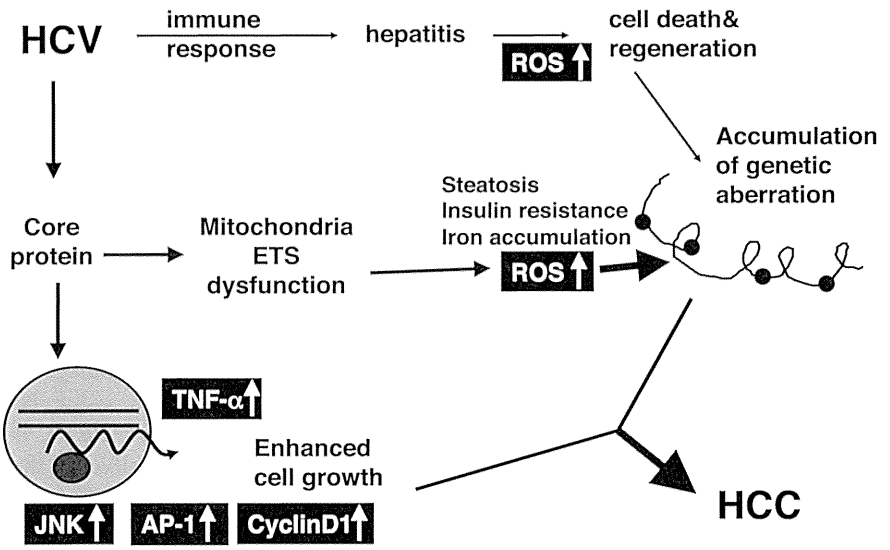

Fig. 2 Molecular pathogenesis of hepatocarcinogenesis in HCV infection. Induction of oxidative stress together with hepatic steatosis by the HCV core protein would play a pivotal role in the development of HCC. Alterations in cellular gene expressions, such as TNF-α, and those in the intracellular signaling pathways including JNK would be co-accelerators to hepatocarcinogenesis in HCV infection. ROS, reactive oxygen species; HCC, hepatocellular carcinoma; TNF-α, tumor necrosis factor-α; JNK, c-Jun N-terminal kinase; AP-1, activating protein-1; ETS, electron transfer system

phosphorylation, and in the response to oxidative stress occurs in HCV-infected human liver with advanced fibrosis (Diamond et al. 2007). Therefore, it is probable that the HCV core protein affects mitochondrial functions, since such pathogenesis is observed in HCV core transgenic mice, cultured cells expressing the core protein (Korenaga et al. 2005), and HCV-infected patients.

The recent progress in proteomics has opened new avenues for disease-related biomarker discovery. We performed a two-dimensional polyacrylamide gel electrophoresis (2D-PAGE) of mitochondria isolated from HepG2 cells stably expressing the HCV core protein and identified several proteins of different expressions when compared with control HepG2 cells. Among upregulated proteins in the core-expressing cells, we focused on prohibitin, which functions as a mitochondrial protein chaperone, and found that the core protein interacts with prohibitin and represses the interaction between prohibitin and subunit proteins of cytochrome C oxidase (COX), which leads to a decrease in the expression level of the proteins and in COX activity.

Prohibitin, a mitochondrial protein chaperone, was identified as an upregulated protein in core-expressing cells. Prohibitin is a ubiquitously expressed and highly conserved protein that was originally determined to play a predominant role in inhibiting cell cycle progression and cellular proliferation by attenuating DNA

synthesis (Mishra et al. 2005). It exists in the nucleus and interacts with transcription factors that are vital in cell cycle progression. In core-expressing cells, prohibitin was also detected in the nucleus, and its expression level was also higher than that in control cells. Mitochondrial prohibitin acts as a protein chaperone by stabilizing newly synthesized mitochondrial translation products through direct interaction (Nijtmans et al. 2000). We examined the interaction between prohibitin and mitochondria-encoded subunit II of COX and found a suppressed interaction between these proteins in core-expressing cells. In addition, there are several studies that showed the association of prohibitin with the assembly of mitochondrial respiratory complex I as well as complex IV (COX) (Nijtmans et al. 2000). Complex I also consists of both nuclear and mitochondrial DNA-encoded subunits; therefore, it is probable that the assembly and function of complex I are impaired by the core protein. With respect to the complex I function, we previously found a decreased complex I activity in core-expressing cells. Other groups have also shown that complex I activity is decreased in cultured cells (Piccoli et al. 2007). From these findings, the interaction between prohibitin and the core protein may impair the function of complex I as well as complex IV, leading to an increase in ROS production. In fact, the suppression of the prohibitin function is shown to result in an increased production of ROS (Theiss et al. 2007), a phenomenon observed in core-expressing cells used in this study as well as in the liver of core gene transgenic mice (Moriya et al. 2001a). Very interestingly, the liver-specific deletion of prohibitin resulted in the morphological abnormality and HCC (Ko et al. 2010).

This is a new mechanism for ROS overproduction in viral infection in that HCV induces mitochondrial dysfunction through the inhibition of chaperone function in the mitochondria (Tsutsumi et al. 2009).

7 HCV not only Induces ROS But Attenuates Some Antioxidant System

As discussed above, chronic hepatitis C is characterized by its prominent augmentation of oxidative stress. Related to this, iron accumulation in the liver has been shown to aggravate the oxidative stress as shown by the increase in the amount of DNA adducts in the liver (Farinati et al. 1995). Iron is accumulated in the liver of the HCV core gene transgenic mice (Moriya et al. 2010). The accumulation of iron observed in the liver of the core gene transgenic mice fed with normal chow corroborates well with the observation in chronic hepatitis C patients (Farinati et al. 1995; Fujita et al. 2008). Then, the impact of iron overloading on the oxidant/antioxidant system was examined using this mouse model and cultured cells. Iron overloading caused the induction of ROS as well as antioxidants. However, some of the key antioxidant enzymes, including HO-1 and NADH dehydrogenase, and quinone 1 (NDQ-1), were not augmented sufficiently by iron overloading, while other antioxidant enzymes such as catalase and GST were

augmented more strongly in the iron-overloaded core gene transgenic mice than in the iron-overloaded control or non-iron-overloaded core gene transgenic mice. The attenuation of iron-induced augmentation of HO-1 was also confirmed in HepG2 cells expressing the core protein. HO-1 catalyzes the initial and rate-limiting reaction in heme catabolism and cleaves pro-oxidant heme to form biliverdin, which is converted to bilirubin in mammals, both of which have been known to have very strong antioxidant activities (Stocker et al. 1987). In addition, HO-1 has been also suggested to be a central antioxidant under the condition of glutathione depletion. Thus, HO-1 is an essential protective endogenous mechanism against oxidative stress, particularly, in the case of iron overload. Therefore, it is probable that the attenuation of HO-1 and NQO-1 would hamper the antioxidant system and lead to a robust production of oxidative stress in HCV infection.

Thus, HCV infection not only induces ROS but also hampers the antioxidant activation in the liver, thereby exacerbating oxidative stress that would facilitate hepatocarcinogenesis. Aggravation of oxidative stress by overloading of iron was also shown using other transgenic mouse lines carrying HCV genome (Nishina et al. 2008).

8 Metabolic Changes in HCV Infection: Co-factor for Liver Disease Progression

Steatosis is frequently observed in chronic hepatitis C patients and significantly associated with accelerated progression rate of fibrosis of the liver (Powell et al. 2005). The composition of fatty acids that are accumulated in the liver of core gene transgenic mice is different from that in fatty liver due to simple obesity. Carbon 18 mono-unsaturated fatty acids (C18:1) such as oleic or vaccenic acid, which favor the proliferation of cancer cells (Kudo et al. 2011), are significantly increased. This is also the case in the comparison of liver tissues from hepatitis C patients and simple fatty liver patients due to obesity (Moriya et al. 2001b).

The mechanism of steatogenesis in hepatitis C was investigated using this mouse model. At least three pathways are involved in the development of steatosis. One is the frequent presence of insulin resistance in hepatitis C patients as well as in the core gene transgenic mice, which occurs through the inhibition of tyrosine phosphorylation of insulin receptor substrate (IRS)-1 (Shintani et al. 2004). Insulin resistance increases the peripheral release and hepatic uptake of fatty acids, resulting in the accumulation of lipid in the liver. The second pathway is the suppression of the activity of microsomal triglyceride transfer protein (MTP) by HCV core protein (Perlemuter et al. 2002). This inhibits the secretion of very-low-density protein (VLDL) from the liver, yielding an increase in triglycerides in the liver. The last one involves the sterol regulatory element–binding protein (SREBP)-1c, which regulates the production of triglycerides and phospholipids. In HCV core gene transgenic mice, SREBP-1c is upregulated, neither SREBP-2 nor SREBP-1a (Moriishi et al. 2007). This corroborates the results of in vitro studies

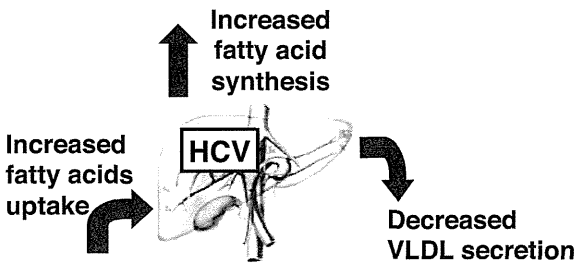

Fig. 3 HCV induces steatosis in the liver by involving three pathways of lipid metabolism. First, HCV core protein induces insulin resistance, leading to the increase in peripheral release and hepatic uptake of fatty acids. Second, HCV core protein suppresses the activity of MTP, inhibiting the secretion VLDL from the liver, yielding an increase in triglycerides in the liver. Lastly, a transcription factor, SREBP-1c, is upregulated by HCV core protein, resulting in an increased production of triglycerides. Thus, the involvement of three pathways easily leads to the development of hepatic steatosis in hepatitis C patients. MTP, microsomal triglyceride transfer protein; VLDL, very-low-density protein; SREBP, sterol regulatory element–binding protein

(Kim et al. 2007; Waris et al. 2007) and a chimpanzee study (Su et al. 2002). Thus, the involvement of three pathways would easily lead to the development of hepatic steatosis in hepatitis C patients (Fig. 3). The presence of steatosis exacerbates the production of ROS and accelerates the progression of liver disease in hepatitis C.

9 Conclusion

The results of HCV mouse studies indicate a carcinogenic activity of the HCV core protein in vivo; thus, HCV would have an oncogenic potential in the liver. In research studies of carcinogenesis, it has been established that the accumulation of a complete set of cellular genetic aberrations is necessary for the development of neoplasia such as colorectal cancer (Kinzler and Vogelstein 1996). They have deduced that mutations in the APC gene for inactivation, those in K-*ras* for activation, and those in the p53 gene for inactivation accumulate, which cooperate toward the development of colorectal cancer. Their theory has been extended to the carcinogenesis of other cancers as well, called "Vogelstein-type" carcinogenesis.

On the basis of the results we obtained for the induction of HCC by the HCV core protein, we would like to present a different mechanism for the hepatocarcinogenesis in HCV infection. We do allow multistages in the induction of all cancers; it would be mandatory for hepatocarcinogenesis that many mutations accumulate in hepatocytes. Some of these steps, however, may be skipped in the development of HCC in HCV infection to which the core protein would contribute. The overall effects achieved by the expression of the viral protein would be the induction of HCC, even in the absence of a complete set of genetic aberrations, required for carcinogenesis (Fig. 4). By considering such a "non-Vogelstein-type" process for the induction of HCC, a reasonable explanation may be given for

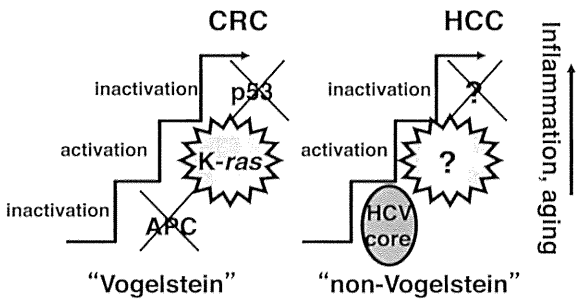

Fig. 4 The role of HCV in hepatocarcinogenesis. Multiple steps are required in the induction of all cancers; it would be mandatory for hepatocarcinogenesis that genetic mutations accumulate in hepatocytes. However, in HCV infection, some of these steps may be skipped in the development of HCC in the presence of the core protein. The effect achieved by the core protein would be one step up in the stairway to HCC, even in the absence of a complete set of genetic aberrations required for carcinogenesis. By considering such a "non-Vogelstein-type" process for the induction of HCC, a reasonable explanation would be given for many unusual modes of hepatocarcinogenesis in hepatitis C, such as a very high incidence and multicentric nature of HCC development. CRC, colorectal cancer; HCC, hepatocellular carcinoma; APC, adenomatous polyposis coli

unusual events happening in HCV carriers (Koike 2005). Now it does not seem so difficult as before to determine why HCC develops in persistent HCV infection at an outstandingly high incidence. Our theory may also give an account of the non-metastatic and multicentric *de novo* occurrence characteristics of HCC, which would be the result of persistent HCV infection.

References

Alonzi T, Agrati C, Costabile B, Cicchini C, Amicone L, Cavallari C, Rocca CD, Folgori A, Fipaldini C, Poccia F, Monica NL, Tripodi M (2004) Steatosis and intrahepatic lymphocyte recruitment in hepatitis C virus transgenic mice. J Gen Virol 85:1509–1520

Boulant S, Montserret R, Hope RG, Ratinier M, Targett-Adams P, Lavergne JP et al (2006) Structural determinants that target the hepatitis C virus core protein to lipid droplets. J Biol Chem 281:22236–22247

Diamond DL, Jacobs JM, Paeper B, Proll SC, Gritsenko MA, Carithers RL Jr et al (2007) Proteomic profiling of human liver biopsies: hepatitis C virus-induced fibrosis and mitochondrial dysfunction. Hepatology 46:649–657

Farinati F, Cardin R, De Maria N, Della Libera G, Marafin C, Lecis E, Burra P, Floreani A, Cecchetto A, Naccarato R (1995) Iron storage, lipid peroxidation and glutathione turnover in chronic anti-HCV positive hepatitis. J Hepatol 22:449–456

Frelin L, Brenndörfer ED, Ahlén G, Weiland M, Hultgren C, Alheim M, Glaumann H, Rozell B, Milich DR, Bode JG, Sällberg M (2006) The hepatitis C virus and immune evasion: non-structural 3/4A transgenic mice are resistant to lethal tumour necrosis factor alpha mediated liver disease. Gut 55:1475–1483

Fujita N, Sugimoto R, Ma N, Tanaka H, Iwasa M, Kobayashi Y, Kawanishi S, Watanabe S, Kaito M, Takei Y (2008) Comparison of hepatic oxidative DNA damage in patients with chronic hepatitis B and C. J Viral Hepat 15:498–507

Honda A, Arai Y, Hirota N, Sato T, Ikegaki J, Koizumi T, Hatano M, Kohara M, Moriyama T, Imawari M, Shimotohno K, Tokuhisa T (1999) Hepatitis C virus structural proteins induce liver cell injury in transgenic mice. J Med Virol 59:281–289

Houghton M, Weiner A, Han J, Kuo G, Choo QL (1991) Molecular biology of hepatitis C viruses. Implications for diagnosis, development and control of viral diseases. Hepatology 14:381–388

Ikeda K, Saitoh S, Suzuki Y, Kobayashi M, Tsubota A, Koida I et al (1998) Disease progression and hepatocellular carcinogenesis in patients with chronic viral hepatitis: a prospective observation of 2215 patients. J Hepatol 28:930–938

Kato J, Kobune M, Nakamura T, Kuroiwa G, Takada K, Takimoto R, Sato Y, Fujikawa K, Takahashi M, Takayama T, Ikeda T, Niitsu Y (2001) Normalization of elevated hepatic 8-hydroxy-2'-deoxyguanosine levels in chronic hepatitis C patients by phlebotomy and low iron diet. Cancer Res 61:8697–8702

Kim KH, Hong SP, Kim K, Park MJ, Kim KJ, Cheong J (2007) HCV core protein induces hepatic lipid accumulation by activating SREBP1 and PPARgamma. Biochem Biophys Res Commun 55:883–888

Kinzler KW, Vogelstein B (1996) Lessons from hereditary colorectal cancer. Cell 87:159–170

Kiyosawa K, Sodeyama T, Tanaka E, Gibo Y, Yoshizawa K, Nakano Y et al (1990) Interrelationship of blood transfusion, non-A, non-B hepatitis and hepatocellular carcinoma: analysis by detection of antibody to hepatitis C virus. Hepatology 12:671–675

Ko KS, Tomasi ML, Iglesias-Ara A, French BA, French SW, Ramani K, Lozano JJ, Oh P, He L, Stiles BL, Li TW, Yang H, Martínez-Chantar ML, Mato JM, Lu SC (2010) Liver-specific deletion of prohibitin 1 results in spontaneous liver injury, fibrosis, and hepatocellular carcinoma in mice. Hepatology 52:2096–2108

Koike K (2005) Molecular basis of hepatitis C virus-associated hepatocarcinogenesis: lessons from animal model studies. Clin Gastroenterol Hepatol 3:S132–S135

Koike K, Moriya K, Ishibashi K, Matsuura Y, Suzuki T, Saito I et al (1995) Expression of hepatitis C virus envelope proteins in transgenic mice. J Gen Virol 76:3031–3038

Koike K, Moriya K, Yotsuyanagi H, Shintani Y, Fujie H, Ishibashi K et al (1997) Sialadenitis resembling Sjögren's syndrome in mice transgenic for hepatitis C virus envelope genes. Proc Natl Acad Sci USA 94:233–236

Korenaga M, Wang T, Li Y, Showalter LA, Chan T, Sun J, Weinman SA (2005) Hepatitis C virus core protein inhibits mitochondrial electron transport and increases reactive oxygen species (ROS) production. J Biol Chem 280:37481–37488

Kudo Y, Tanaka Y, Tateishi K, Yamamoto K, Yamamoto S, Mohri D, Isomura Y, Seto M, Nakagawa H, Asaoka Y, Tada M, Ohta M, Ijichi H, Hirata Y, Otsuka M, Ikenoue T, Maeda S, Shiina S, Yoshida H, Nakajima O, Kanai F, Omata M, Koike K (2011) Altered composition of fatty acids exacerbates hepatotumorigenesis during activation of the phosphatidylinositol 3-kinase pathway. J Hepatol 55:1400–1408

Lerat H, Honda M, Beard MR, Loesch K, Sun J, Yang Y et al (2002) Steatosis and liver cancer in transgenic mice expressing the structural and nonstructural proteins of hepatitis C virus. Gastroenterology 122:352–365

Machida K, Cheng KT, Lai CK, Jeng KS, Sung VM, Lai MM (2006) Hepatitis C virus triggers mitochondrial permeability transition with production of reactive oxygen species, leading to DNA damage and STAT3 activation. J Virol 80:7199–7207

Majumder M, Ghosh AK, Steele R, Zhou XY, Phillips NJ, Ray R, Ray RB (2002) Hepatitis C virus NS5A protein impairs TNF-mediated hepatic apoptosis, but not by an anti-FAS antibody, in transgenic mice. Virology 294:94–105

Mishra S, Murphy LC, Nyomba BL, Murphy LJ (2005) Prohibitin: a potential target for new therapeutics. Trends Mol Med 11:192–197

Miyamoto H, Moriishi K, Moriya K, Murata S, Tanaka K, Suzuki T et al (2007) Hepatitis C virus core protein induces insulin resistance through a PA28γ-dependent pathway. J Virol 81:1727–1735

Miyoshi H, Fujie H, Shintani Y, Tsutsumi T, Shinzawa S, Makuuchi M, Kokudo N, Matsuura Y, Suzuki T, Miyamura T, Moriya K, Koike K (2005) Hepatitis C virus core protein exerts an inhibitory effect on suppressor of cytokine signaling (SOCS)-1 gene expression. J Hepatol 43:757–763

Moradpour D, Penin F, Rice CM (2007) Replication of hepatitis C virus. Nat Rev Microbiol 5:453–463

Moriishi K, Okabayashi T, Nakai K, Moriya K, Koike K, Murata S et al (2003) Proteasome activator PA28 gamma-dependent nuclear retention and degradation of hepatitis C virus core protein. J Virol 77:10237–10249

Moriishi K, Mochizuki R, Moriya K, Miyamoto H, Mori Y, Abe T et al (2007) Critical role of PA28g in hepatitis C virus-associated steatogenesis and hepatocarcinogenesis. Proc Natl Acad Sci USA 104:1661–1666

Moriya K, Yotsuyanagi H, Shintani Y, Fujie H, Ishibashi K, Matsuura Y et al (1997) Hepatitis C virus core protein induces hepatic steatosis in transgenic mice. J Gen Virol 78:1527–1531

Moriya K, Fujie H, Shintani Y, Yotsuyanagi H, Tsutsumi T, Matsuura Y et al (1998) Hepatitis C virus core protein induces hepatocellular carcinoma in transgenic mice. Nat Med 4:1065–1068

Moriya K, Nakagawa K, Santa T, Shintani Y, Fujie H, Miyoshi H et al (2001a) Oxidative stress in the absence of inflammation in a mouse model for hepatitis C virus-associated hepatocarcinogenesis. Cancer Res 61:4365–4370

Moriya K, Todoroki T, Tsutsumi T, Fujie H, Shintani Y, Miyoshi H et al (2001b) Increase in the concentration of carbon 18 monounsaturated fatty acids in the liver with hepatitis C: analysis in transgenic mice and humans. Biophys Biochem Res Commun 281:1207–1212

Moriya K, Miyoshi H, Shinzawa S, Tsutsumi T, Fujie H, Goto K, Shintani Y, Yotsuyanagi H, Koike K (2010) Hepatitis C virus core protein compromises iron-induced activation of antioxidants in mice and HepG2 cells. J Med Virol 82:776–792

Naas T, Ghorbani M, Alvarez-Maya I, Lapner M, Kothary R, De Repentigny Y et al (2005) Characterization of liver histopathology in a transgenic mouse model expressing genotype 1a hepatitis C virus core and envelope proteins 1 and 2. J Gen Virol 86:2185–2196

Nijtmans LG, de Jong L, Artal Sanz M, Coates PJ, Berden JA, Back JW et al (2000) Prohibitins act as a membrane-bound chaperone for the stabilization of mitochondrial proteins. EMBO J 19:2444–2451

Nishina S, Hino K, Korenaga M, Vecchi C, Pietrangelo A, Mizukami Y, Furutani T, Sakai A, Okuda M, Hidaka I, Okita K, Sakaida I (2008) Hepatitis C virus-induced reactive oxygen species raise hepatic iron level in mice by reducing hepcidin transcription. Gastroenterology 134:226–238

Pasquinelli C, Shoenberger JM, Chung J et al (1997) Hepatitis C virus core and E2 protein expression in transgenic mice. Hepatology 25:719–727

Perlemuter G, Sabile A, Letteron P, Vona G, Topilco A, Koike K et al (2002) Hepatitis C virus core protein inhibits microsomal triglyceride transfer protein activity and very low density lipoprotein secretion: a model of viral-related steatosis. FASEB J 16:185–194

Perz JF, Armstrong GL, Farrington LA, Hutin YJ, Bell BP (2006) The contributions of hepatitis B virus and hepatitis C virus infections to cirrhosis and primary liver cancer worldwide. J Hepatol 45:529–538

Piccoli C, Scrima R, Quarato G, D'Aprile A, Ripoli M, Lecce L et al (2007) Hepatitis C virus protein expression causes calcium-mediated mitochondrial bioenergetic dysfunction and nitro-oxidative stress. Hepatology 46:58–65

Powell EE, Jonsson JR, Clouston AD (2005) Steatosis: co-factor in other liver diseases. Hepatology 42:5–13

Saito I, Miyamura T, Ohbayashi A, Harada H, Katayama T, Kikuchi S et al (1990) Hepatitis C virus infection is associated with the development of hepatocellular carcinoma. Proc Natl Acad Sci USA 87:6547–6549

Shintani Y, Fujie H, Miyoshi H, Tsutsumi T, Kimura S, Moriya K et al (2004) Hepatitis C virus and diabetes: direct involvement of the virus in the development of insulin resistance. Gastroenterology 126:840–848

Shirakura M, Murakami K, Ichimura T, Suzuki R, Shimoji T, Fukuda K et al (2007) E6AP ubiquitin ligase mediates ubiquitylation and degradation of hepatitis C virus core protein. J Virol 81:1174–1185

Suzuki R, Sakamoto S, Tsutsumi T, Rikimaru A, Tanaka K, Shimoike T et al (2005) Molecular determinants for subcellular localization of hepatitis C virus core protein. J Virol 79:1271–1281

Stocker R, Yamamoto Y, McDonagh AF, Glazer AN, Ames BN (1987) Bilirubin is an antioxidant of possible physiological importance. Science 235:1043–1046

Su AI, Pezacki JP, Wodicka L, Brideau AD, Supekova L, Thimme R et al (2002) Genomic analysis of the host response to hepatitis C virus infection. Proc Natl Acad Sci USA 99:15669–15674

Taguwa S, Kambara H, Fujita N, Noda T, Yoshimori T, Koike K, Moriishi K, Matsuura Y (2011) Dysfunction of autophagy participates in vacuole formation and cell death in cells replicating hepatitis C virus. J Virol 85:13185–13194

Theiss AL, Idell RD, Srinivasan S, Klapproth JM, Jones DP, Merlin D et al (2007) Prohibitin protects against oxidative stress in intestinal epithelial cells. FASEB J 21:197–206

Tsutsumi T, Suzuki T, Moriya K, Yotsuyanagi H, Shintani Y, Fujie H et al (2002) Intrahepatic cytokine expression and AP-1 activation in mice transgenic for hepatitis C virus core protein. Virology 304:415–424

Tsutsumi T, Suzuki T, Moriya K, Shintani Y, Fujie H, Miyoshi H et al (2003) Hepatitis C virus core protein activates ERK and p38 MAPK in cooperation with ethanol in transgenic mice. Hepatology 38:820–828

Tsutsumi T, Matsuda M, Aizaki H, Moriya K, Miyoshi H, Fujie H, Shintani Y, Yotsuyanagi H, Miyamura T, Suzuki T, Koike K (2009) Proteomics analysis of mitochondrial proteins reveals overexpression of a mitochondrial protein chaperone, prohibitin, in cells expressing hepatitis C virus core protein. Hepatology 50:378–386

Wakita T, Taya C, Katsume A et al (1998) Efficient conditional transgene expression in hepatitis C virus cDNA transgenic mice mediated by the Cre/loxP system. J Biol Chem 273:9001–9006

Waris G, Felmlee DJ, Negro F, Siddiqui A (2007) Hepatitis C virus induces proteolytic cleavage of sterol regulatory element binding proteins and stimulates their phosphorylation via oxidative stress. J Virol 81:8122–8130

Yotsuyanagi H, Shintani Y, Moriya K, Fujie H, Tsutsumi T, Kato T et al (2000) Virological analysis of non-B, non-C hepatocellular carcinoma in Japan: frequent involvement of hepatitis B virus. J Infect Dis 181:1920–1928

SCIENTIFIC REPORTS

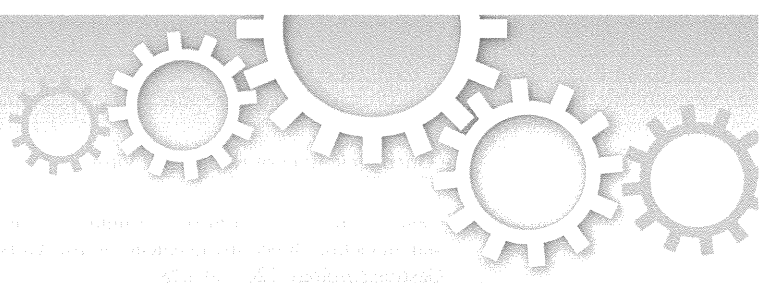

OPEN

SUBJECT AREAS:
MIRNAS
NUTRIENT SIGNALLING
NATURAL PRODUCTS
TYPE 2 DIABETES MELLITUS

Received
10 May 2013

Accepted
15 August 2013

Published
30 August 2013

Correspondence and requests for materials should be addressed to M.O. (otsukamo-tky@umin.ac.jp)

* These authors contributed equally to this work.

The flavonoid apigenin improves glucose tolerance through inhibition of microRNA maturation in miRNA103 transgenic mice

Motoko Ohno[1]*, Chikako Shibata[1]*, Takahiro Kishikawa[1], Takeshi Yoshikawa[1], Akemi Takata[1], Kentaro Kojima[1], Masao Akanuma[2], Young Jun Kang[3], Haruhiko Yoshida[1], Motoyuki Otsuka[1,4] & Kazuhiko Koike[1]

[1]Department of Gastroenterology, Graduate School of Medicine, The University of Tokyo, Tokyo 113-8655, Japan, [2]Division of Gastroenterology, The Institute for Adult Diseases, Asahi Life Foundation, Tokyo 100-0005, Japan, [3]Department of Immunology and Microbial Sciences, The Scripps Research Institute, La Jolla, CA 92037, USA, [4]Japan Science and Technology Agency, PRESTO, Kawaguchi, Saitama 332-0012, Japan.

Polyphenols are representative bioactive substances with diverse biological effects. Here, we show that apigenin, a flavonoid, has suppressive effects on microRNA (miRNA) function. The effects were mediated by impaired maturation of a subset of miRNAs, probably through inhibition of the phosphorylation of TRBP, a component of miRNA-generating complexes via impaired mitogen-activated protein kinase (MAPK) Erk activation. While glucose intolerance was observed in miRNA103 (miR103)-overexpressing transgenic mice, administration of apigenin improved this pathogenic status likely through suppression of matured miR103 expression levels. These results suggest that apigenin may have favorable effects on the pathogenic status induced by overexpression of miRNA103, whose maturation is mediated by phosphorylated TRBP.

Polyphenols, common components of many popular drinks and foods, and caffeine, an alkaloid in various seeds and leaves, are representative bioactive substances with diverse biological effects[1,2]. However, while some effects have been examined in detail[3], the molecular mechanisms underlining these biological effects are mostly undetermined.

MicroRNAs (miRNAs) are short, single-stranded, non-coding RNAs expressed in most organisms ranging from plants to vertebrates[4]. Primary miRNAs, which possess stem-loop structures, are processed into mature miRNAs by Drosha, Dicer, RNA polymerase III, and other related molecules. These mature miRNAs then bind the RNA-induced silencing complex (RISC), and the resulting co-complex directly binds the 3′-untranslated regions (3′-UTRs) of target mRNAs to act as suppressors of translation and gene expression. Thus, dependent upon the identity of the target mRNAs, miRNAs are responsible for the control of various biological functions, including cell proliferation, apoptosis, differentiation, metabolism, oncogenesis, and oncogenic suppression[5–9]. For example, it was reported recently that expression of miRNA103 and 107 (miR103 and 107) was upregulated in obese mice, and that the gain of miR103 function in either liver or fat was sufficient to induce impaired glucose homeostasis[10].

Because the effects of bioactive substances are diverse and the functions of miRNAs result in diverse biological consequences, we hypothesized that some effects of bioactive substances may depend on modulation of miRNA function. In this study, we examined whether polyphenols and caffeine affect miRNA function and determined the molecular mechanisms underlying these effects. In addition, we applied the results obtained here to clinically relevant models to facilitate their use in practical applications.

Results

Apigenin suppresses miRNA function. To determine the effects of polyphenols and caffeine on miRNA function, we determined the luciferase activities of several types of reporters constructed containing

miRNA-binding sites (the function of which is suppressed by corresponding miRNAs) upon treatment with caffeine or polyphenols. The polyphenols used here were apigenin, procyanidin A2 and procyanidin B2 from flavonoids, and chlorogenic acid from phenolic acid. A cell line derived from the liver, Huh7, was used because substances in food theoretically flow into the liver first through the portal vein immediately after intestinal absorption. Among the bioactive substances examined, only apigenin significantly inhibited the effects of miRNAs such as miR122, miR185 and miR103 (Figure 1a), which are highly expressed in the liver[11]. The effects were similarly observed irrespective of endogenous miRNAs or exogenous overexpression of corresponding miRNAs (Figure 1a and b) in a dose-dependent manner (Figure 1c). Another liver cell line, Hep3B, showed similar results, suggesting that the effects were not cell line-specific (Supplementary Figure 1a, b and c). The effects were detected with 5 μM apigenin; this concentration is physiologically attainable[12–14]. These results suggest that apigenin has suppressive effects on miRNA function.

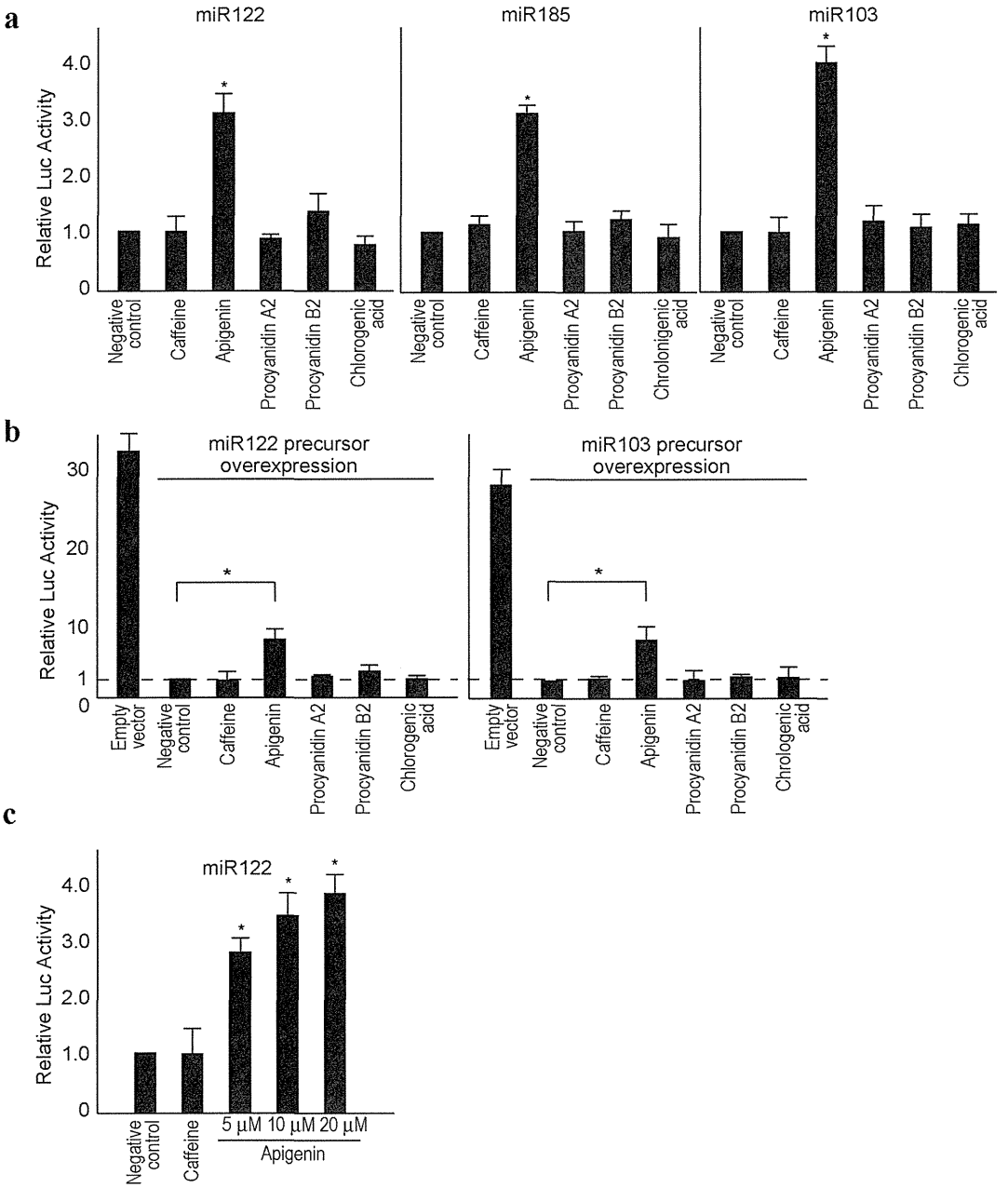

Figure 1 | Apigenin inhibits miRNA function. (a), Apigenin inhibits endogenous miRNA function. Huh7 cells were transfected with reporters to determine the functions of the indicated miRNAs. Twenty-four hours after treatment with the indicated substances, reporter assays were performed. Data represent the means ± standard deviation (s.d.) from three independent experiments. *, $p < 0.05$ (*t*-test). (b), Apigenin inhibits the function of exogenously overexpressed miRNAs. Huh7 cells were transfected with reporters and corresponding miRNA precursor-expressing plasmids or an empty vector. Twenty-four hours after treatment with the indicated substances, reporter assays were performed. Data represent the means ± s.d. from three independent experiments. *, $p < 0.05$ (*t*-test). (c), Dose-dependent effects of apigenin on miRNA function. Huh7 cells were transfected with reporter plasmids to determine miR122 function. Cells were treated with indicated doses of apigenin for 24 h and luciferase assays were performed. Caffeine was included as a negative control. Data represent the means ± s.d. from three independent experiments. *, $p < 0.05$ (*t*-test) compared with the negative control.

Apigenin inhibits miRNA maturation from miRNA precursors. To elucidate the molecular mechanisms underlying the inhibitory effects of apigenin on miRNA function, we first determined the expression levels of miRNA pathway-related molecules including Drosha, DGCR8, KSRP, Argonaute 2 (Ago2), and Dicer in the presence of apigenin. While the expression levels of Drosha, Ago2 and Dicer proteins appeared to decrease slightly after a high dose of apigenin, no significant changes were observed in the expression levels of these proteins (Figure 2a and Supplementary Figure 2a). Next, we examined the expression and maturation of miRNAs by quantitative real-time polymerase chain reaction (qRT-PCR) and Northern blotting (Figure 2b and Supplementary Figure 2b). Expression levels of mature endogenous miR122, miR103, and miR185 decreased and accumulation of precursor miRNAs was also observed after apigenin treatment (Figure 2b), suggesting that maturation from miRNA precursors was decreased. In addition, a comprehensive miRNA microarray analysis confirmed that apigenin altered the expression levels of a major subset of miRNAs (Supplementary Figure 2c; the raw data were deposited in the GEO database; GSE46526). However, some miRNAs, such as let-7, were not affected by apigenin treatment, which was confirmed by qRT-PCR (Figure 2b). These results suggest that apigenin has an inhibitory effect on the maturation of a subset of miRNAs.

Apigenin inhibits phosphorylation of TRBP. The microRNA-generating complex is composed of Dicer and phospho-TRBP isoforms[15], and TRBP phosphorylation enhances the maturation of a subset of miRNAs through stabilization of the microRNA-generating complexes[15]. Phosphorylation of TRBP is mediated by mitogen-activated protein kinase (MAPK) Erk[15]. Because apigenin is known to inhibit Erk activity[16–19], we hypothesized that the inhibitory effects of apigenin on miRNA maturation may be mediated by decreased phosphorylation of TRBP through inhibition of Erk. Consistent with previous reports, although caffeine had no effect on the Erk phosphorylation status, apigenin clearly inhibited Erk phosphorylation 24 h post-treatment without changes in total Erk levels (Figure 3a). Concordantly, SRE-driven reporter activities were diminished by apigenin treatment (Figure 3b), suggesting that apigenin indeed inhibited an Erk-mediated intracellular signaling pathway, consistent with previous reports[16–19]. While TRBP was phosphorylated under normal serum culture conditions, and its phosphorylation status did not change with caffeine treatment, its phosphorylation was inhibited by apigenin (Figure 3c). This effect was confirmed by electrophoresis in a phos-tag gel, which showed a clear slow-migrating band, indicating that TRBP was phosphory lated in control and caffeine-treated conditions, but its phosphorylation was inhibited upon treatment with apigenin (Figure 3d). To confirm that Erk activity was inhibited by apigenin following TRBP phosphorylation, we examined the effects of apigenin using Huh7 cells stably expressing constitutively active Mek1 (CA-MEK) on TRBP phosphorylation. As shown in Figure 3e, the degree of TRBP phosphorylation was increased only by CA-MEK expression, and the augmented phosphorylation was not diminished by apigenin treatment (Figure 3e), suggesting that the effects of apigenin could not be observed under the induced Erk activation. That is, the effects of apigenin were most probably mediated by inhibition of Erk activation. In addition, we established Huh7 cells stably expressing dominant negative Erk (DN-Erk). As predicted, the levels of mature miRNA103, 122, and 185, were decreased in DN-Erk expressing cells, but were slightly increased in CA-MEK expressing cells, irrespective of apigenin treatment (Figure 3f). The expression levels of mature let-7, which were examined as a representative miRNA that was not affected by apigenin treatment in the miRNA microarray (Figure 3f), were not changed by enforced expression of DN-Erk or CA-MEK, suggesting that this miRNA maturation is not significantly regulated by MAPK activity or TRBP phosphorylation, consistent with a previous report[15]. These results suggest that apigenin inhibits Erk phosphorylation, and subsequent decreased MAPK activity leads to a decrease in TRBP phosphorylation, which may result in decreased maturation of a subset of miRNAs.

Apigenin improves glucose tolerance through inhibition of miRNA function. To apply the above results in a clinical setting, we focused on recent findings demonstrating that a gain of miR103/107 expression induces impaired glucose homeostasis *in vivo*[10]. To utilize this, we generated transgenic mice expressing a miR103 precursor under control of the CMV promoter (Supplementary Figure 3a). Overexpression of miR103 in these mice was confirmed by Northern blotting against mature miR103 in liver tissues (Figure 4a and Supplementary Figure 3b). No significant over-saturation of RISC

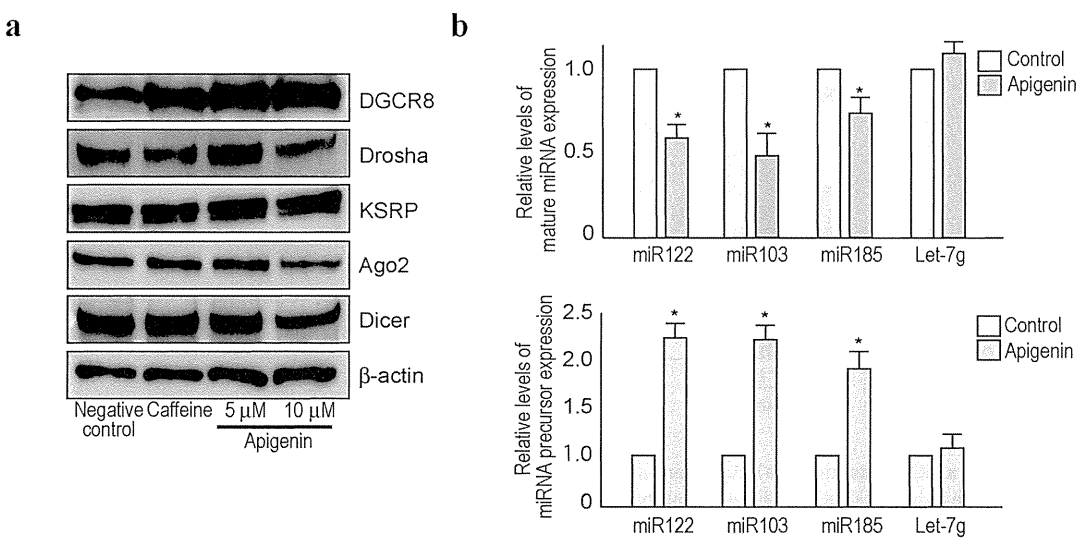

Figure 2 | Apigenin impairs miRNA maturation. (a), Cells were treated with the appropriate substances for 24 h and the indicated proteins were blotted. Representative results from three independent experiments using Huh7 cells are shown. Full-length blot images are available in Supplementary Figure 5a. (b), The expression levels of mature miRNAs and miRNA precursors were determined by qRT-PCR using Huh7 cells with or without apigenin treatment for 24 h. Data represent the means ± s.d. from three independent experiments. *, $p < 0.05$ (*t*-test) compared with the control (DMSO only) treatment.

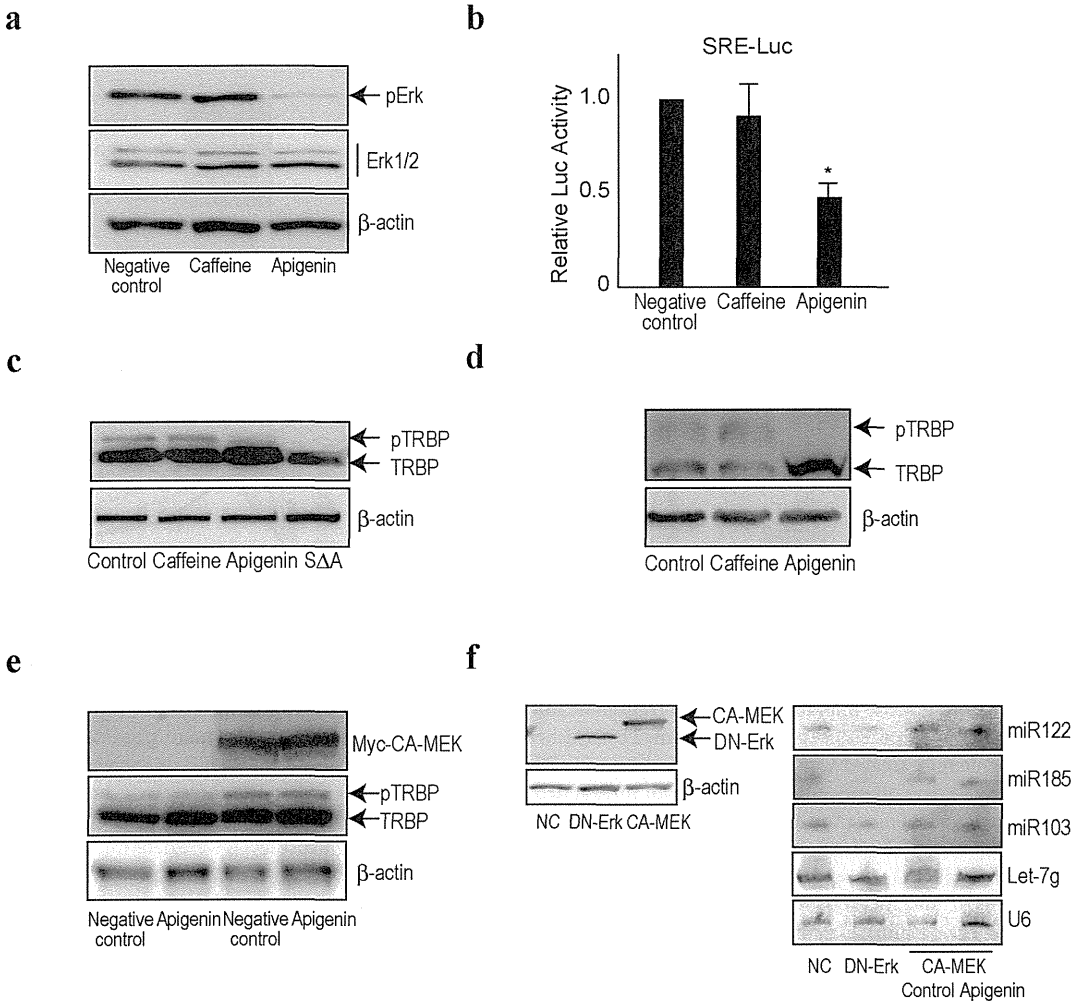

Figure 3 | Apigenin inhibits TRBP phosphorylation. (a), Cells were treated with caffeine or apigenin for 24 h. Cell lysates were blotted with anti-phosphorylated Erk and anti-total Erk1/2. Representative results from three independent experiments using Huh7 cells are shown. Similar results were obtained using Hep3B cells. (b), A luciferase assay was performed to determine SRE-driven transcription under apigenin treatment. Caffeine was included as a comparison. Data represent the means ± s.d. from three independent experiments using Huh7 cells. *, $p < 0.05$ (*t*-test) compared to the negative control. (c), Huh7 cells were transfected with wild-type TRBP-expressing plasmids followed by treatment with the indicated substances for 24 h. Serine-to-alanine mutant TRBP (SΔA) indicates non-phosphorylated TRBP. Representative results from three independent experiments using Huh7 cells are shown. (d), Substance-treated Huh7 cell lysates were separated using a Mn2+-Phos-tag gel to discriminate the phosphorylated form of TRBP. Representative results from three independent experiments using Huh7 cells are shown. (e), TRBP-expressing Huh7 cells were stably transfected with myc-tagged CA-MEK-expressing plasmids followed by apigenin treatment for 24 h. Phosphorylation status of TRBP was determined by Western blotting. Representative results from three independent experiments are shown. (f), Huh7 cells were stably transfected with myc-tagged CA-MEK-expressing plasmids or myc-tagged DN-Erk-expressing plasmids. The expression of the transfected constructs was confirmed by Western blotting using anti-myc antibodies (left panels). Expression levels of mature miRNAs in those cells with or without apigenin treatment were determined by Northern blotting (right panels). Representative results of at least three independent experiments are shown. Full-length blot images in a, b, c, d, e, and f are available in Supplementary Figure 5b, c, d, e, and f.

complexes due to overexpressing miR103 in these mice was confirmed by a lack of significant changes in the expression levels of other mature miRNAs, such as miR122 and miR185 (Figure 4a). As expected from a previous report[10], these miR103 transgenic mice showed an increase in both random and fasting blood-glucose levels and insulin levels (Supplementary Figure 3c and d). The mean size of adipocytes in visceral fat was larger in normal chow fed miR103 transgenic mice than in control mice, and their size became larger nearly in parallel in both control and miR103 transgenic mice under a high-fat diet (Supplementary Figure 3e).

To determine the effect of apigenin in these models, 40 mg/kg apigenin was intraperitoneally injected daily for 14 days in miR103 transgenic mice. The level of mature miR103 was decreased, and precursors accumulated in apigenin-treated mice, as determined by Northern blotting and qRT-PCR (Figure 4b and Supplementary Figure 4a and b). Similar to the in vitro results, levels of mature miR122 and miR185, but not let-7, in the liver tissues were also decreased by apigenin treatment (Supplementary Figure 4a and b). Phosphorylated TRBP in the liver tissues was decreased in apigenin-treated mice, as determined by a retarded band in the phos-tag gel (Figure 4c), consistent with the *in vitro* results (Figure 3d). Erk phosphorylation was consistently decreased following apigenin treatment (Supplementary Figure 4c). In addition, we confirmed the upregulated expression level of caveolin-1, a major regulator of the insulin receptor, which is a direct target gene of miR103[10] in these tissues (Supplementary Figure 4c). As expected from these results, apigenin-treated miR103 transgenic mice showed decreased random and fasting blood glucose-levels (Figure 4d). While miR103 transgenic mice

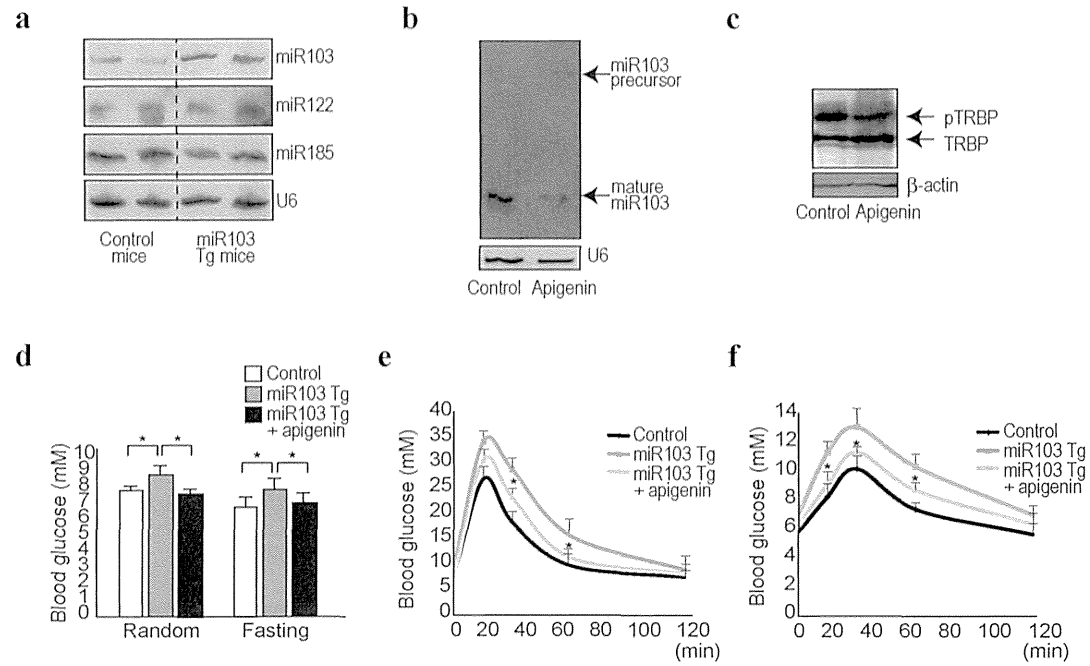

Figure 4 | Apigenin improves glucose tolerance in miR103 transgenic mice. (a), Expression levels of mature miR103, miR122, and miR185 in liver tissues of miR103 transgenic mice (miR103 Tg) were determined by Northern blotting. (b), Expression levels of mature miR103 and its precursor in liver tissues of miR10-transgenic mice treated with apigenin were determined by Northern blotting. Control (DMSO) or apigenin (40 mg/kg) was injected intraperitoneally daily for 14 days. Representative results from three independent mouse sets are shown. (c), Liver tissue homogenates from miR103 transgenic mice were separated using a phos-tag gel to determine the phosphorylation status of TRBP. Representative results from three independent mouse sets are shown. Full-length blot image is available in Supplementary Figure 5g. (d), Blood glucose levels were determined at random times or after 12 h fasting in control and miR103 transgenic (miR103 Tg) mice (n = 8 in each group). Data represent the means ± s.d. *, $p < 0.05$ (*t*-test). (e), (f), Glucose and pyruvate tolerance tests in control, miR103 transgenic (miR103 Tg), and miR103 transgenic with apigenin treatment (miR103 Tg + apigenin) mice (n = 6 in each group). Data represent the means ± s.d. *, $p < 0.05$ (*t*-test).

showed impaired glucose tolerance after an intraperitoneal glucose injection, apigenin treatment significantly suppressed these phenomena (Figure 4e). Similarly, while miR103 transgenic mice showed increased glucose production during an intraperitoneal pyruvate-tolerance test, apigenin treatment also suppressed these effects (Figure 4f). In addition, an increased number of small adipocytes and a decreased number of large adipocytes were observed in apigenin-treated miR103 transgenic mice (Supplementary Figure 3e and f). These results suggest that apigenin may have beneficial effects on pathological conditions in miR103 transgenic mice.

Discussion

In this study, we demonstrated that apigenin (4′,5,7-trihydroxyflavone) has inhibitory effects on the maturation processes of a subset of miRNAs and subsequent miRNA function. These effects may be mediated through inhibition of TRBP phosphorylation, possibly through inhibition of Erk activation. These results suggest that apigenin may be utilized to improve miRNA-mediated pathogenic states, such as glucose tolerance, induced by the over-expression of miRNA103.

Bioactive substances, such as caffeine and polyphenols, have been reported to have pleiotropic physiological effects[3,20]. However, those phenomena are descriptive in most cases and the underlying mechanisms are largely unclear. Apigenin, which is present in many fruits and vegetables, also has diverse biological effects, including improvement of the cancer cell response to chemotherapy[21], tumorigenesis[13,22], modulating immune cell function[23], and anti-platelet activity[24]. In this study, we showed that apigenin inhibits TRBP phosphorylation and its related miRNA maturation through inhibition of MAPK Erk activation. This modulation of miRNA function by apigenin may account, at least in part, for its various reported biological effects.

Phosphorylation of TRBP is mediated by Erk[15]. We showed clear inhibition of Erk phosphorylation by apigenin. Although previous studies have reported the inhibition of Erk activation by apigenin[16–19], the underlying mechanisms were unknown. Because Erk has many biological functions in intracellular signaling, modulation of TRBP phosphorylation and miRNA expression induced by Erk inhibition through apigenin is likely a part of the phenotype. To clarify the biological function of apigenin, identification of molecules on which apigenin directly acts must be the next step.

Another important finding in this study was the impaired glucose tolerance observed in miR103 transgenic mice. Previous studies showed that recombinant adenoviruses expressing the miR103/107 family (only one nucleotide difference in miR103 and miR107 at position 21) and a gain of miR103/107 function by transient infection in mice was sufficient to induce impaired glucose homeostasis, and these miRNAs play a central role in insulin sensitivity[10]. In this study, we confirmed that constitutive expression of miR103 in mice resulted in impaired glucose tolerance and increased size of adipocytes. These mice may represent a new *in vivo* model of metabolic disorders and facilitate development of new drugs targeting impaired glucose tolerance. In fact, we found that apigenin reversed impaired glucose tolerance in miR103-transgenic mice. Because apigenin is one of the flavonoids and is present in high content in celery and parsley, intake of apigenin from foods or dietary supplements may have some favorable effects on glucose intolerance induced by overexpression of miRNA levels, even if it does not completely overcome impaired glucose tolerance.

Phosphorylated TRBP is not related to the maturation of all miRNAs, but rather a subset of miRNAs[15]. With this respect, apigenin may have favorable effects on the pathogenic status induced by overexpression or overfunction of the miRNAs to which phosphorylated TRBP is related. Maturation of miR122, a liver-specific miRNA, is at least partly regulated by apigenin, as shown in our study, its crucial function in cholesterol synthesis[11,25–28], and hepatitis c viral replication[29,30]. Therefore, apigenin may also have beneficial effects on these conditions. Other effects of apigenin on the pathological state may be necessary to reconsider from the point of view of overexpression or overfunction of specific miRNAs.

Simultaneously, one should be cautious about the modulation of miRNA function by apigenin. Because some miRNAs may have favorable effects on human health, apigenin might be harmful if it inhibits the maturation and function of such miRNAs. For example, inhibitory effects on tumor-suppressive miRNAs should be avoided. Caution regarding these issues is necessary and, in parallel, the biological functions of miRNAs in general should be further examined.

In summary, we showed that apigenin displays inhibitory effects on the phosphorylation of TRBP and its subsequent miRNA maturation and function through regulation of Erk activity. Decreasing miRNA function may be used for treatment of conditions induced by over-functioning of miRNAs. Moreover, clarifying the as-yet-undiscovered functions of bioactive substances is important. Similar strategies to those used here may also be applied to other bioactive substances whose effects have been reported but the mechanisms are as yet undetermined.

Methods

Cell culture. The human hepatocellular carcinoma cell lines, Huh7 and Hep3B, were obtained from the Japanese Collection of Research Bioresources (JCRB, Osaka, Japan). All cells were maintained in Dulbecco's modified Eagle's medium supplemented with 10% fetal bovine serum.

Reagents. Caffeine, apigenin and chlorogenic acid were purchased from Wako Chemicals (Osaka, Japan). Procyanidin A2 and B2 were purchased from Indofine Chemical (Hillsborough, NJ) and ChromaDex (Irvine, CA). Caffeine, chlorogenic acid and procyanidin B2 were dissolved in water. Apigenin and procyanidin A2 were dissolved in dimethyl sulfoxide (DMSO). Caffeine, chlorogenic acid and procyanidin A2 and B2 were added at concentrations of 20 μM, 10 μM, 50 μg/mL, and 50 μg/mL, respectively, as reported previously[31–34]. Apigenin was used at 10 μM unless otherwise specified for *in vitro* studies, and 40 mg/kg was used for intraperitoneal injection daily for *in vivo* studies. An equal volume of DMSO only was used as a negative control.

Mouse experiments. Experimental protocols were approved by the Ethics Committee for Animal Experimentation at the Graduate School of Medicine, the University of Tokyo and the Institute for Adult Disease, Asahi Life Foundation, Japan and conducted in accordance with the Guidelines for the Care and Use of Laboratory Animals of the Department of Medicine, the University of Tokyo, and the Institute for Adult Disease, Asahi Life Foundation.

Plasmids, transfection and dual luciferase assays. Plasmids expressing miR122 and miR185 precursors and the corresponding firefly luciferase-based reporters have been described previously[8,35]. Plasmids expressing miRNA-103 precursors and the corresponding luciferase reporter were newly constructed according to protocols reported previously[8]. To determine MAPK pathway activity, SRE-driven luciferase was transfected, and dual luciferase assays were performed as described previously[9], with the exception that pGL4.74, a control plasmid containing *Renilla reniformis* (sea pansy) luciferase under control of the herpes simplex virus thymidine kinase promoter (Promega), was used as an internal control. Chemicals were added at 24 h and the reporter assays were done 48 h post-transfection. Constitutively active MEK1(DD) and dominant negative Erk(K/N) constructs with zeocin resistance genes were kindly provided by Prof. Takekawa (The Institute of Medical Sciences, the University of Tokyo)[36]. After transfection, the cells were selected with 6 μg/mL zeocin to establish cells stably expressing those constructs.

Western blot analysis. Protein lysates were prepared from cells or mouse liver tissues for immunoblotting analyses. Western blotting was performed as described previously[8]. Primary antibodies were purchased from Sigma (DGCR8, #SAB4200088; Dicer, #SAB4200087; TRBP2, #SAB4200111; β-actin, #A5441), Bethyl (KSRP, A302-021), Wako (Ago2, 015-22031), and Cell Signaling (Drosha, #D28B1; Phospho-Erk, #9101; Total Erk, #4695; myc-tag, #2276; Caveolin, #3267).

Northern blotting of miRNAs. Northern blotting of miRNAs was performed as described previously[9]. Briefly, total RNA was extracted using TRIzol Reagent (Invitrogen, Carlsbad, CA) according to the manufacturer's instructions. Ten micrograms of RNA were resolved in denaturing 15% polyacrylamide gels containing 7 M urea in 1× TBE and then transferred to a Hybond N+ membrane (GE Healthcare) in 0.25× TBE. Membranes were UV-crosslinked and prehybridized in hybridization buffer. Hybridization was performed overnight at 42°C in ULTRAhyb-Oligo Buffer (Ambion) containing a biotinylated probe specific for miR122 (CAA ACA CCA TTG TCA CAC TCC A), miR103 (TCA TAG CCC TGT ACA ATG CTG CT), miR185 (TCA GGA ACT GCC TTT CTC TCC A), and let-7g (AAC TGT ACA AAC TAC TAC CTC A), which had been heated to 95°C for 2 min. Membranes were washed at 42°C in 2× SSC containing 0.1% SDS, and the bound probe was visualized using a BrightStar BioDetect Kit (Ambion). Blots were stripped by boiling in a solution containing 0.1% SDS and 5 mM EDTA for 10 min prior to rehybridization with a U6 probe (CAC GAA TTT GCG TGT CAT CCT T).

Quantitative RT-PCR analysis of miRNA expression. To determine miR122, miR103, miR185, and let-7g expression levels, cDNA was first synthesized from RNA, and quantitative PCR was then performed using Mir-X miRNA First-Strand Synthesis and SYBR qRT-PCR Kit (Clontech). The expression levels of miRNA precursor were determined according to the previous report[37] using the reported primers. Relative expression values were calculated by the *CT*-based calibrated standard curve method. These calculated values were then normalized to the expression of U6 snRNA. The reverse primer was provided in the kit.

Determining TRBP phosphorylation status. Plasmids expressing wild-type TRBP and kinase-dead TRBP (TRBP SΔA) were kindly provided by Professor Liu[15]. Twenty-four hours after transfection into Huh7 cells with corresponding plasmids, substances were treated for 24 h, and cell lysates were collected for subsequent Western blotting. To better discriminate the phosphorylated form of TRBP from the unphosphorylated form, a Mn2+-Phos-tag SDS-PAGE gel (Wako) was used according to the manufacturer's instructions.

Generation of miR103-expressing transgenic mice. To construct transgenic mice, plasmids expressing miRNA-103 precursors were modified as follows: to add the SV40 poly(A) tail signal downstream of the miR103 precursor sequences, the pCDH-miR103 precursor-expressing plasmid was digested at the *Not*I restriction site, and PCR-amplified poly(A) tail signal sequences were digested with *Cla*I from the original plasmid as a template was inserted by the Infusion cloning system (Clontech, Mountain View, CA). A DNA fragment of 1,125 bp, containing the CMV promoter region, the 470-bp genomic region for the miR103 precursor, and a SV40 poly(A) tail signal, was resected from the constructed plasmid by digestion with *Cla*I. Stable C57BL/6 embryonic stem (ES) cell lines were generated by electroporation of the linearized transgene, and the resulting cells were injected into blastocysts by the UNITECH Company (Chiba, Japan). Genotyping was performed by PCR using DNA isolated from tail snips. Four different mouse lines were maintained and the male littermates were used in the experiments.

Glucose test. Blood glucose was tested using a Glucose Pilot system (Iwai Chemical, Japan). Glucose tolerance and pyruvate tolerance tests were performed by intraperitoneal injection of glucose (2 g/kg) or pyruvate (2 g/kg) after fasting overnight. Blood glucose levels were measured before injection (0 min) and at 15, 30, 60, and 120 min after injection.

Adipocyte size. Visceral fat tissues stained with hematoxylin and eosin were analyzed using the Image-J software. One hundred adipocytes were measured per animal to determine adipocyte size. The high-fat diet was purchased from CLEA-Japan (Tokyo, Japan).

miRNA microarray analyses. miRNA microarray analysis was performed using miRNA oligo chips (Toray Industries, Tokyo, Japan). Normalization was performed using the intensities from U6, instead of the standard global normalization. The data and the protocols were deposited in a public database (Please refer the following link during the review process; http://www.ncbi.nlm.nih.gov/geo/query/acc.cgi?token=frwpxomkicoicte&acc=GSE46526).

Statistical analysis. Statistically significant differences between groups were determined using Student's *t*-test when variances were equal. When variances were unequal, Welch's *t*-test was used. *P*-values less than 0.05 were considered to indicate statistical significance.

1. Surh, Y. J. Cancer chemoprevention with dietary phytochemicals. *Nat Rev Cancer* **3**, 768–780 (2003).
2. D'Incalci, M., Steward, W. P. & Gescher, A. J. Use of cancer chemopreventive phytochemicals as antineoplastic agents. *Lancet Oncol* **6**, 899–904 (2005).
3. Baur, J. A. *et al.* Resveratrol improves health and survival of mice on a high-calorie diet. *Nature* **444**, 337–342 (2006).
4. Carrington, J. & Ambros, V. Role of microRNAs in plant and animal development. *Science* **301**, 336–338 (2003).
5. Bartel, D. P. MicroRNAs: genomics, biogenesis, mechanism, and function. *Cell* **116**, 281–297 (2004).
6. Ambros, V. The functions of animal microRNAs. *Nature* **431**, 350–355 (2004).

7. Lu, J. *et al.* MicroRNA expression profiles classify human cancers. *Nature* **435**, 834–838 (2005).
8. Kojima, K. *et al.* MicroRNA122 is a key regulator of α-fetoprotein expression and influences the aggressiveness of hepatocellular carcinoma. *Nat Commun* **2**, 338 (2011).
9. Takata, A. *et al.* MicroRNA-140 acts as a liver tumor suppressor by controlling NF-κB activity by directly targeting DNA methyltransferase 1 (Dnmt1) expression. *Hepatology* **57**, 162–170 (2013).
10. Trajkovski, M. *et al.* MicroRNAs 103 and 107 regulate insulin sensitivity. *Nature* **474**, 649–653 (2011).
11. Krützfeldt, J. *et al.* Silencing of microRNAs in vivo with 'antagomirs'. *Nature* **438**, 685–689 (2005).
12. Budhraja, A. *et al.* Apigenin induces apoptosis in human leukemia cells and exhibits anti-leukemic activity in vivo. *Mol Cancer Ther* **11**, 132–142 (2012).
13. Shukla, S. *et al.* Blockade of beta-catenin signaling by plant flavonoid apigenin suppresses prostate carcinogenesis in TRAMP mice. *Cancer Res* **67**, 6925–6935 (2007).
14. Wang, W. *et al.* Cell-cycle arrest at G2/M and growth inhibition by apigenin in human colon carcinoma cell lines. *Mol Carcinog* **28**, 102–110 (2000).
15. Paroo, Z., Ye, X., Chen, S. & Liu, Q. Phosphorylation of the human microRNA-generating complex mediates MAPK/Erk signaling. *Cell* **139**, 112–122 (2009).
16. Yi Lau, G. T. & Leung, L. K. The dietary flavonoid apigenin blocks phorbol 12-myristate 13-acetate-induced COX-2 transcriptional activity in breast cell lines. *Food Chem Toxicol* **48**, 3022–3027 (2010).
17. Tatsuta, A. *et al.* Suppression by apigenin of peritoneal metastasis of intestinal adenocarcinomas induced by azoxymethane in Wistar rats. *Clin Exp Metastasis* **18**, 657–662 (2000).
18. Yin, F., Giuliano, A. E. & Van Herle, A. J. Signal pathways involved in apigenin inhibition of growth and induction of apoptosis of human anaplastic thyroid cancer cells (ARO). *Anticancer Res* **19**, 4297–4303 (1999).
19. Kuo, M. L. & Yang, N. C. Reversion of v-H-ras-transformed NIH 3T3 cells by apigenin through inhibiting mitogen activated protein kinase and its downstream oncogenes. *Biochem Biophys Res Commun* **212**, 767–775 (1995).
20. Yao, S. L. *et al.* Selective radiosensitization of p53-deficient cells by caffeine-mediated activation of p34cdc2 kinase. *Nat Med* **2**, 1140–1143 (1996).
21. Chan, L. P. *et al.* Apigenin induces apoptosis via tumor necrosis factor receptor- and Bcl-2-mediated pathway and enhances susceptibility of head and neck squamous cell carcinoma to 5-fluorouracil and cisplatin. *Biochim Biophys Acta* **1820**, 1081–1091 (2012).
22. Mafuvadze, B., Liang, Y., Besch-Williford, C., Zhang, X. & Hyder, S. M. Apigenin induces apoptosis and blocks growth of medroxyprogesterone acetate-dependent BT-474 xenograft tumors. *Horm Cancer* **3**, 160–171 (2012).
23. Nicholas, C. *et al.* Apigenin blocks lipopolysaccharide-induced lethality in vivo and proinflammatory cytokines expression by inactivating NF-kappaB through the suppression of p65 phosphorylation. *J Immunol* **179**, 7121–7127 (2007).
24. Landolfi, R., Mower, R. L. & Steiner, M. Modification of platelet function and arachidonic acid metabolism by bioflavonoids. Structure-activity relations. *Biochem Pharmacol* **33**, 1525–1530 (1984).
25. Hsu, S. H. *et al.* Essential metabolic, anti-inflammatory, and anti-tumorigenic functions of miR-122 in liver. *J Clin Invest* **122**, 2871–2883 (2012).
26. Lanford, R. E. *et al.* Therapeutic silencing of microRNA-122 in primates with chronic hepatitis C virus infection. *Science* **327**, 198–201 (2010).
27. Elmén, J. *et al.* LNA-mediated microRNA silencing in non-human primates. *Nature* **452**, 896–899 (2008).
28. Esau, C. *et al.* miR-122 regulation of lipid metabolism revealed by in vivo antisense targeting. *Cell Metab* **3**, 87–98 (2006).
29. Jopling, C. L., Yi, M., Lancaster, A. M., Lemon, S. M. & Sarnow, P. Modulation of hepatitis C virus RNA abundance by a liver-specific MicroRNA. *Science* **309**, 1577–1581 (2005).
30. Lindow, M. & Kauppinen, S. Discovering the first microRNA-targeted drug. *J Cell Biol* **199**, 407–412 (2012).
31. Ku, B. M. *et al.* Caffeine inhibits cell proliferation and regulates PKA/GSK3β pathways in U87MG human glioma cells. *Mol Cells* **31**, 275–279 (2011).
32. Nishizuka, T. *et al. Procya* nidins are potent inhibitors of LOX-1: a new player in the French Paradox. *Proc Jpn Acad Ser B Phys Biol Sci* **87**, 104–113 (2011).
33. Teraoka, M. *et al.* Cytoprotective effect of chlorogenic acid against α-synuclein-related toxicity in catecholaminergic PC12 cells. *J Clin Biochem Nutr* **51**, 122–127 (2012).
34. Shukla, S. & Gupta, S. Apigenin: a promising molecule for cancer prevention. *Pharm Res* **27**, 962–978 (2010).
35. Takata, A. *et al.* MicroRNA-22 and microRNA-140 suppress NF-κB activity by regulating the expression of NF-κB coactivators. *Biochem Biophys Res Commun* **411**, 826–831 (2011).
36. Kubota, Y., O'Grady, P., Saito, H. & Takekawa, M. Oncogenic Ras abrogates MEK SUMOylation that suppresses the ERK pathway and cell transformation. *Nat Cell Biol* **13**, 282–291 (2011).
37. Suzuki, H. I. *et al. Modulat* ion of microRNA processing by p53. *Nature* **460**, 529–533 (2009).

Acknowledgments

This work was supported by Grants-in-Aid from the Ministry of Education, Culture, Sports, Science and Technology, Japan (#25293076 and #24390183) (to M. Otsuka and K. Koike), by Health Sciences Research Grants of The Ministry of Health, Labor and Welfare of Japan (to K. Koike), and grants from the Nestlé Nutrition Council, Japan (to A.T.), and the Foundation of All Japan Coffee Association (to M. Otsuka).

Author contributions

M.Ohno, C.S. and M.Otsuka planned the research and wrote the paper. M.Ohno, C.S., T.K., T.Y., A.T., K.Kojima, and M.Otsuka performed the majority of the experiments. M.A. and H.Y. contributed materials. Y.K. supported several experiments. K.Koike supervised the entire project.

Additional information

Supplementary information accompanies this paper at http://www.nature.com/scientificreports

Competing financial interests: The authors declare no competing financial interests.

How to cite this article: Ohno, M. *et al.* The flavonoid apigenin improves glucose tolerance through inhibition of microRNA maturation in miRNA103 transgenic mice. *Sci. Rep.* 3, 2553; DOI:10.1038/srep02553 (2013).

Research Article

EASL EUROPEAN ASSOCIATION FOR THE STUDY OF THE LIVER | JOURNAL OF HEPATOLOGY

A genome-wide association study of HCV-induced liver cirrhosis in the Japanese population identifies novel susceptibility loci at the MHC region

Yuji Urabe[1,2], Hidenori Ochi[2], Naoya Kato[4], Vinod Kumar[1,3], Atsushi Takahashi[3], Ryosuke Muroyama[4], Naoya Hosono[3], Motoyuki Otsuka[5], Ryosuke Tateishi[5], Paulisally Hau Yi Lo[1], Chizu Tanikawa[1], Masao Omata[5], Kazuhiko Koike[5], Daiki Miki[2], Hiromi Abe[2], Naoyuki Kamatani[3], Joji Toyota[6], Hiromitsu Kumada[7], Michiaki Kubo[3], Kazuaki Chayama[2], Yusuke Nakamura[1,3], Koichi Matsuda[1,*]

[1]*Laboratory of Molecular Medicine, Human Genome Center, Institute of Medical Science, The University of Tokyo, Tokyo, Japan;* [2]*Department of Medical and Molecular Science, Division of Frontier Medical Science, Programs for Biomedical Research, Graduate School of Biomedical Sciences, Hiroshima University, Hiroshima, Japan;* [3]*Center for Genomic Medicine, The Institute of Physical and Chemical Research (RIKEN), Kanagawa, Japan;* [4]*Unit of Disease Control Genome Medicine, The Institute of Medical Science, The University of Tokyo, Tokyo, Japan;* [5]*Department of Gastroenterology, Graduate School of Medicine, The University of Tokyo, Tokyo, Japan;* [6]*Department of Gastroenterology, Sapporo Kosei General Hospital, Hokkaido, Japan;* [7]*Department of Hepatology, Toranomon Hospital, Tokyo, Japan*

Background & Aims: We performed a genome-wide association study (GWAS) of hepatitis C virus (HCV)-induced liver cirrhosis (LC) to identify predictive biomarkers for the risk of LC in patients with chronic hepatitis C (CHC).

Methods: A total of 682 HCV-induced LC cases and 1045 CHC patients of Japanese origin were genotyped by Illumina Human Hap 610-Quad bead Chip.

Results: Eight SNPs which showed possible associations ($p < 1.0 \times 10^{-5}$) at the GWAS stage were further genotyped using 936 LC cases and 3809 CHC patients. We found that two SNPs within the major histocompatibility complex (MHC) region on chromosome 6p21, rs910049 and rs3135363, were significantly associated with the progression from CHC to LC ($p_{combined} = 9.15 \times 10^{-11}$ and 1.45×10^{-10}, odds ratio (OR) = 1.46 and 1.37, respectively). We also found that *HLA-DQA1*0601* and *HLA-DRB1*0405* were associated with the progression from CHC to LC ($p = 4.53 \times 10^{-4}$ and 1.54×10^{-4} with OR = 2.80 and 1.45, respectively). Multiple logistic regression analysis revealed that rs3135363, rs910049, and *HLA-DQA1*0601* were independently associated with the risk of HCV-induced LC. In addition, individuals with four or more risk alleles for these three loci have a 2.83-fold higher risk for LC than those with no risk allele, indicating the cumulative effects of these variations.

Conclusions: Our findings elucidated the crucial roles of multiple genetic variations within the MHC region as prognostic/predictive biomarkers for CHC patients.

Introduction

Two million people in Japan and 210 million people worldwide are estimated to be infected with the hepatitis C virus (HCV), which is known to be a major cause of chronic viral liver disease [1]. Patients with chronic hepatitis C (CHC) usually exhibit mild inflammatory symptoms, but are at a significantly high risk for developing liver cirrhosis (LC) and hepatocellular carcinoma [2]. More than 400,000 people at present suffer from LC, which is ranked as the 9th major cause of death in Japan. In addition, liver cancer causes approximately 32,000 deaths per year, making it the 4th most common cause of death from malignant diseases. Thus, HCV-related diseases are important public health problems [3].

Clinical outcomes after the exposure to HCV vary enormously among individuals. Approximately 70% of infected persons will develop chronic hepatitis [4], and about 20–30% of CHC patients will develop cirrhosis, but others can remain asymptomatic for decades [2]. The annual death rate of patients with decompensated cirrhosis is as high as 15–30% [5]. Moreover, more than 7% of LC patients develop hepatocellular cancer in Japan and Taiwan, while the frequencies are less than 1.6% among other ethnic groups [6,7]. These inter-individual and inter-ethnic differences have been attributed to various factors such as viral genotypes,

Keywords: Genome-wide association study; Hepatitis C virus; Liver cirrhosis; Major histocompatibility complex.

Received 22 April 2012; received in revised form 15 December 2012; accepted 24 December 2012; available online 12 January 2013

* Corresponding author. Address: Laboratory of Molecular Medicine, Institute of Medical Science, The University of Tokyo, 4-6-1 Shirokanedai, Minato, Tokyo 108-8639, Japan. Tel.: +81 3 5449 5376; fax: +81 3 5449 5123.

E-mail address: koichima@ims.u-tokyo.ac.jp (K. Matsuda).

Abbreviations: CHC, chronic hepatitis C; GWAS, genome-wide association study; HCV, hepatitis C virus; LC, liver cirrhosis; MHC, major histocompatibility complex; OR, odds ratio; PBC, primary biliary cirrhosis; SNPs, single nucleotide polymorphisms.

ELSEVIER

Journal of Hepatology **2013** vol. 58 | 875–882

Table 1. Characteristics of samples and methods used in this study.

Stage	Source	Platform	Number of samples	Female (%)	Age, yr (mean ± SD)
GWAS					
Liver cirrhosis	BioBank Japan	Illumina Human Hap 610	682	313 (46.3)	67.1 ± 9.7
Chronic hepatitis C[a]	Hiroshima University	Illumina Human Hap 610	1045	371 (35.5)	55.2 ± 11.0
Replication					
Liver cirrhosis	Tokyo University	Invader assay	716	334 (46.8)	64.4 ± 10.4
	Hiroshima University		220	98 (44.5)	64.7 ± 8.98
Chronic hepatitis C[a]	BioBank Japan	Invader assay	1670	780 (46.8)	59.7 ± 12.6
	Hiroshima University		2139	1061 (51.8)	58.8 ± 9.20

[a]Number of samples that qualified. CHC patients with severe liver fibrosis (F3 or F4) or lower platelet counts (<160,000) were excluded.

alcohol consumption, age at infection, co-infection of HIV or HBV [8–10], insulin resistance, steatosis, and metabolic syndrome [11]. Previous gene expression analyses also identified various genes associated with liver fibrosis among patients with CHC [12–14]. In addition, miRNAs such as mir-21 and mir-122 were shown to be correlated with live fibrosis [15,16].

Currently, the genome-wide association study is the most common method to identify genetic variations associated with disease risk [17–20]. In addition, the roles of genetic factors in HCV-related diseases have been elucidated. *IL28B* is associated with spontaneous clearance of HCV [21] as well as with the clinical response to the combination therapy of pegylated interferon and ribavirin [22,23]. Recently, our group has shown that SNP rs2596542 on *MICA* [24] and SNP rs1012068 on *DEPDC5* [25] are significantly associated with HCV-induced liver cancer. Although liver cirrhosis is the major risk factor of liver cancer, a fraction of CHC patients will develop HCC without accompanying LC. Therefore, the underlying genetic background would be different between HCV-induced LC and HCV-induced HCC. Previous studies identified the association of genetic variants in *HLA-DQ/DR/B* [26–28], *2–5AS* [29], *TLR3* [30], and *PNPLA3* [31] with the risk of liver fibrosis among patients with CHC. However, a comprehensive approach for HCV-induced LC has not been conducted so far. Here we performed GWAS of HCV-induced LC to identify predictive biomarkers for the risk of LC in patients with CHC.

Materials and methods

Ethics statement

All subjects provided written informed consent. This project was approved by the ethical committees at University of Tokyo, Hiroshima University, Sapporo Kosei General Hospital, Toranomon Hospital, and Center for Genomic Medicine, Institutes of Physical and Chemical Research (RIKEN).

Study population

The characteristics of each cohort are shown in Table 1. In this study, we conducted GWAS and replication analysis on a total of 1618 HCV-induced LC and 4854 CHC patients. All subjects had abnormal levels of serum alanine transaminase for more than 6 months and were positive for both HCV antibody and serum HCV RNA. Among 1618 LC and 4854 CHC samples, 342 LC patients (21.14%) and 2997 CHC patients (61.70%) underwent liver biopsy. The remaining 1276 LC and 1857 CHC patients were diagnosed by non-invasive methods including hepatic imaging (e.g., ultrasonography, computed tomography, arteriography or magnetic resonance imaging), biochemical data (serum bilirubin, serum albumin, platelet, or prothrombin time), and the presence/absence of clinical manifestations of portal hypertension (e.g., varices, encephalopathy or ascites). The patients with CHC or LC were recruited for this study regardless of their treatment history. We excluded from the analysis the followings CHC patients: (1) advanced liver fibrosis (F3 or F4 by New Inuyama classification) [32], (2) platelet count under 160,000 for patients without liver fibrosis staging, and (3) HBV co-infection. Characteristics of each study cohort are shown in Table 1. In brief, DNA of HCV-induced LC and CHC patients was obtained from Biobank Japan (http://biobankjp.org/) [33], the Hiroshima Liver Study Group (http://home.hiroshima-u.ac.jp/naika1/researchprofile/pdf/liverstudygroupe.pdf), Toranomon Hospital, and the University of Tokyo. All subjects were of Japanese origin.

SNP genotyping

Genomic DNA was extracted from peripheral blood leukocytes using a standard method. In GWAS, we genotyped 682 LC and 1045 CHC samples using Illumina Human Hap 610-Quad bead Chip (Supplementary Fig. 1). Samples with low call rate (<0.98) were excluded from our analysis (six LC and two CHC samples). We then applied SNP quality control as follows: call rate $\geqslant$0.99 in LC and CHC samples, Hardy–Weinberg $p \geqslant 1 \times 10^{-6}$ in LC and CHC samples. Consequently, 461,992 SNPs on the autosomal chromosomes passed the quality control filters. SNPs with minor allele frequency of <0.01 in both LC and CHC samples were excluded from further analyses, considering statistical power in the replication analysis. Finally, we analyzed 431,618 SNPs in GWAS. Among the top ten SNPs showing $p < 1.0 \times 10^{-5}$, we selected nine SNPs for further analysis with LD threshold of $r^2 = 0.95$. In the replication stage, we genotyped 936 LC and 3809 CHC using multiplex PCR-based Invader assay (Third Wave Technologies).

Statistical analysis

The association of SNPs with the phenotype in the GWAS, replication stage, and combined analyses was tested by logistic regression analysis, upon adjusting for age at recruitment (continuous) and gender, by assuming additive model using PLINK [34]. In the GWAS, the genetic inflation factor λ was derived by applying logistic regressed p values for all the tested SNPs. The quantile–quantile plot was drawn using R program. The odds ratios were calculated using the non-susceptible allele as reference, unless stated otherwise. The combined analysis of GWAS and replication stage was verified by using the Mantel–Haenszel method. We set the significance threshold as follows; $p = 1 \times 10^{-5}$ in the GWAS stage (first stage) and $p = 6.25 \times 10^{-3}$ (=0.05/8) in the replication analysis. We considered $p < 5 \times 10^{-8}$ as threshold of GWAS significance in the combined analysis, which is the Bonferroni-corrected threshold for the number of independent SNPs genotyped in HapMap Phase II [35]. The heterogeneity across two stages was examined by using the Breslow–Day test [36]. We used Haploview software to analyze the association of haplotypes and LD values between SNPs. Quality control for SNPs was applied as follows: call rate $\geqslant$0.95 in LC and CHC samples, and Hardy–Weinberg $p \geqslant 1 \times 10^{-6}$ in CHC samples in replication stage. The statistical power was 19.51% in GWAS (the first stage) ($p = 1.00 \times 10^{-5}$), 97.98% in replication ($p = 0.05/8$), and 74.76% in the combined stage ($p = 5.00 \times 10^{-8}$) at minor allele frequency of 0.3 and OR of 1.3.

Imputation-based association analysis of HLA class I and class II alleles

We obtained an SNP or a combination of SNPs which could tag the HLA alleles in the Japanese population from a previous study [37]. Genotypes of tagging SNPs were imputed in the GWAS samples by using a Hidden Markov model programmed in MACH [38] and haplotype information from HapMap JPT samples

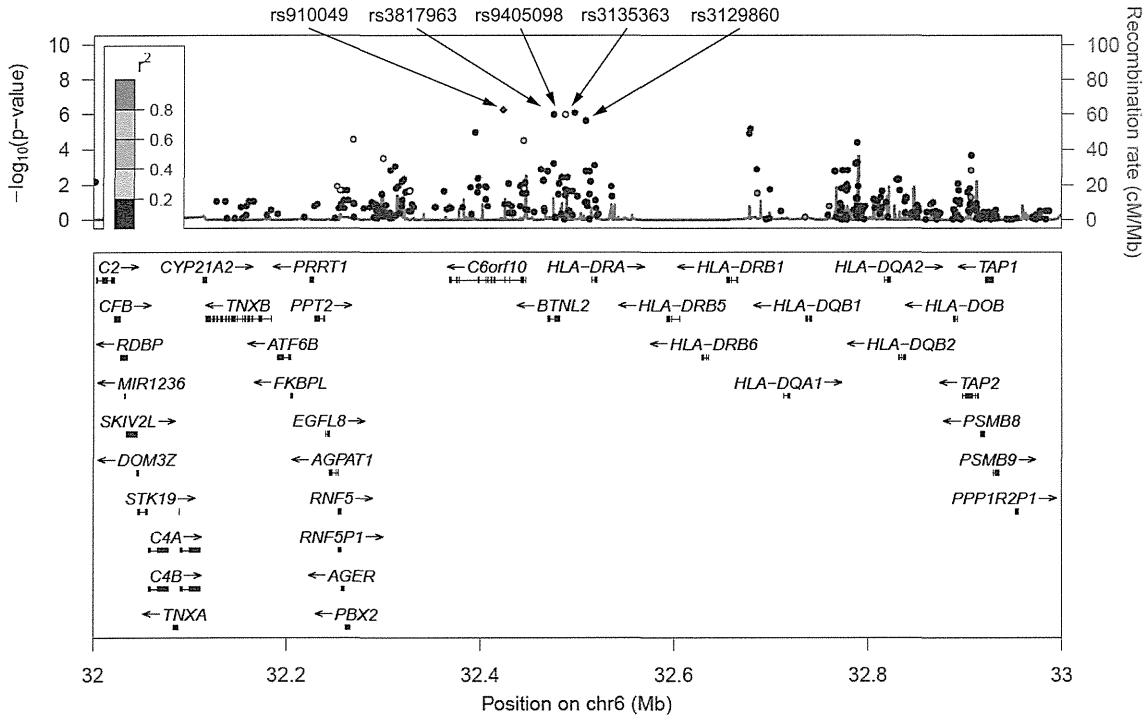

Fig. 1. Regional association plot at 6p21.3. (Upper panel) p Values of genotyped SNPs (circle) and imputed SNPs (cross) are plotted (as $-\log_{10} p$ value) against their physical position on chromosome 6 (NCBI Build 36). The p value for rs910049 at GWAS is represented by a purple diamond. Estimated recombination rates from HapMap JPT show the local LD structure. Inset; the color of the other SNPs indicates LD with rs3135363 according to a scale from $r^2 = 0$ to $r^2 = 1$ based on pair-wise r^2 values from HapMap JPT. (Lower panel) Gene annotations from the University of California Santa Cruz genome browser.

and 1000 genome imputation samples [39]. We applied the same SNP quality criteria as in GWAS, to select SNPs for the analysis. We employed the logistic regression analysis upon age and gender adjustment to assess the associations between HCV-induced LC and HLA alleles.

Software

For general statistical analysis, we employed R statistical environment version 2.9.1 (cran.r-project.org) or plink-1.06 (pngu.mgh.harvard.edu/~purcell/plink/). The Haploview software version 4.2 [40] was used to calculate LD and to draw Manhattan plot. Primer3 -web v0.3.0 (http://frodo.wi.mit.edu) web tool was used to design primers. We employed LocusZoom (http://csg.sph.umich.edu/locuszoom/) for regional plots. We used SNP Functional Prediction web tool for functional annotation of SNPs (http://snpinfo.niehs.nih.gov/snpfunc.htm) [41]. We used "Gene Expression Analysis Based on Imputed Genotypes" (http://www.sph.umich.edu/csg/liang/imputation) [42] for eQTL analysis. We used MACTH [43] web tool for searching potential binding sites for transcription factors (http://www.gene-regulation.com/index.htm).

Results

Genome-wide association study for HCV-induced liver cirrhosis

We performed a two-stage GWAS using a total of 1618 cases and 4854 controls (Supplementary Fig. 1). In the first stage, a whole genome scan was performed on 682 Japanese patients with HCV-induced LC and 1045 Japanese patients with CHC, using Illumina Human Hap 610-Quad bead Chip. The genotyping results of 431,618 single nucleotide polymorphisms (SNPs) obtained after our standard quality control were used for further analysis. CHC patients with severe liver fibrosis (F3 or F4 according to the New Inuyama classification [32]) or lower platelet counts (<160,000) were excluded from the control group. As progression from CHC to LC is strongly affected by age and gender, we performed logistic regression analyses including age and gender as covariates at all tested loci in our analyses. The genetic inflation factor lambda was 1.051, indicating that there is little or no evidence of population stratification (Supplementary Fig. 2A). Although no SNPs cleared the GWAS significance threshold ($p < 5 \times 10^{-8}$) at the first stage, we selected ten candidate SNPs showing suggestive association of $p < 1 \times 10^{-5}$ (Supplementary Fig. 2B and Supplementary Table 1). After excluding SNP rs6891116 due to almost absolute linkage with SNP rs10252674 ($r^2 = 0.99$), the remaining nine SNPs were further genotyped using an independent cohort, consisting of 936 LC and 3809 CHC cases, by multiplex PCR-based Invader assay as the second stage. We could successfully obtain genotype results for eight SNPs after the QC filter (call rate $\geqslant 0.95$ in LC and CHC samples, Hardy–Weinberg of $p \geqslant 1 \times 10^{-6}$ in CHC samples). The logistic regression analysis adjusted by age and gender revealed that five SNPs on chromosome 6q21.3 indicated a significant association with progression from CHC to LC after the Bonferroni correction ($p < 0.05/8 = 6.25 \times 10^{-3}$, Supplementary Table 2). A meta-analysis of the two stages with a fixed-effects model revealed that all of the five SNPs significantly associated with progression from CHC to LC (p values of 9.15×10^{-11}–1.28×10^{-8} with odds ratios (OR) of 1.30–1.46, Fig. 1 and Table 2). These five SNPs were located in the HLA class II region and were in strong linkage disequilibrium with each other (D' >0.75,